Available online at www.sciencedirect.com
SCIENCE DIRECT®
International Journal of Mass Spectrometry 228 (2003) 191–207
International Journal of Mass Spectrometry
www.elsevier.com/locate/ijms

The distinctive behavior of isomeric methyl ethyl mixed esters of 2-methylmaleic acid upon electron ionization

T. Tamiri[a,b], J. Ben Ari[a], S. Zitrin[b], A. Mandelbaum[a,*]

[a] *Lise Meitner—Minerva Center for Computational Quantum Chemistry, Technion—Israel Institute of Technology, Department of Chemistry, Haifa 32 000, Israel*
[b] *Division of Identification and Forensic Science (DIFS), Israel Police, Jerusalem 91906, Israel*

Received 21 November 2002; accepted 17 March 2003

Dedicated to Helmut Schwarz, great friend, man and scientist, on the occasion of his 60th birthday.

Abstract

Isomeric mixed methyl ethyl esters of 2-methylmaleic acid (citraconic acid) show different electron ionization (EI) mass spectra. Methyl radical is exclusively lost from the $M^{\bullet+}$ ion of one isomer ((*Z*)-methyl 3-ethoxycarbonyl-2-butenoate), while the elimination of methanol is more efficient in the other ((*Z*)-ethyl 3-methoxycarbonyl-2-butenoate). Mechanistic pathways have been proposed for these two specific reactions based on the results of deuterium labeling and collision-induced dissociation (CID) studies. The initial step in both fragmentation processes is the hydrogen transfer from position 2 of the ethoxy group to the oxygen atom of the adjacent carbonyl. The proposed ion structures and mechanistic pathways were supported by theoretical calculations using hybrid B3LYP density functional (DFT) method with the 6-31G(d,p) basis set.

Keywords: Electron ionization (EI); Mass spectra of isomers; Collision-induced dissociation (CID); Ion structures; Mechanism of fragmentation; Deuterium labeling; DFT calculations; Citraconates; Esters

1. Introduction

We have previously shown that electron ionization (EI) and chemical ionization (CI) mass spectra enable clear differentiation between closely-related isomers, such as methyl ethyl esters of maleic and substituted succinic acids, differing in the position of the methyl and ethyl groups [1–9]. This makes mass spectrometry a method of choice for the identification of such isomers, which exhibit similar IR and NMR spectra.

The different behavior of such isomers may result in the discovery of new unexpected mechanistic pathways of fragmentation of gas phase ions. One such case is the highly specific dehalogenation in 2-chloro- and bromosuccinates [6]. Only one of the two isomeric ethyl methyl esters in this system, namely that with the ethyl group at position 4, distant from the halogen atom, **1a**, gives rise to a very abundant *m*/*z* 159 $[M - \text{halogen}]^+$ ion upon EI. A detailed study showed that this seemingly simple dissociation of **1a** is in fact a stepwise process, which involves at least two site specific hydrogen migrations, one from position 2 of the ethoxy group to the carbonyl oxygen atom, and the other from C3 of the succinic moiety to

* Corresponding author. Tel.: +972-4-8233-735; fax: +972-4-829-5703.
E-mail address: chr17am@techunix.technion.ac.il (A. Mandelbaum).

1387-3806/$ – see front matter
doi:10.1016/S1387-3806(03)00209-4

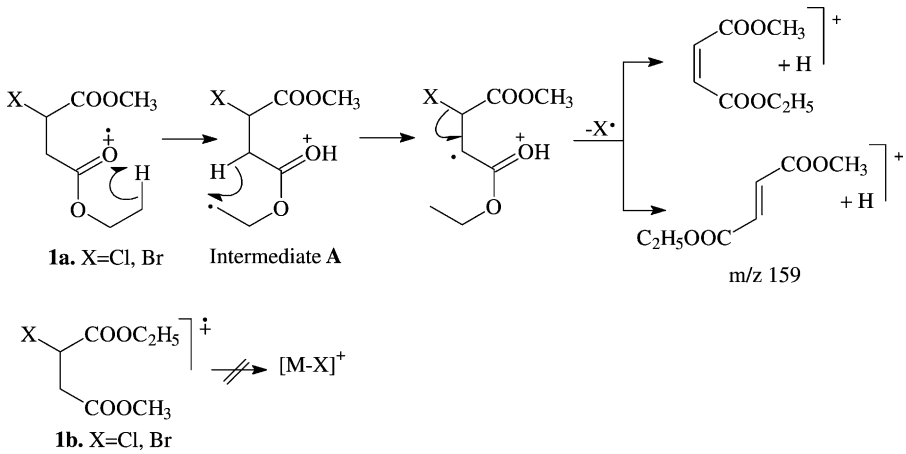

Scheme 1.

the radical site formed at C2 of the original ethoxyl [3]. The proposed mechanism for this dehalogenation, leading to the mixture of protonated maleate and fumarate (as indicated by a collision-induced dissociation (CID) study), is shown in Scheme 1.

In the course of the examination of the behavior of isomeric mixed esters we found that the isomeric ethyl methyl citraconates **2a** and **2b** ((*Z*)-methyl 3-ethoxycarbonyl-2-butenoate and (*Z*)-ethyl 3-methoxycarbonyl-2-butenoate, respectively) give rise to significantly different mass spectra under EI. The major points of difference are the elimination of methanol and the loss of a methyl radical from the $M^{\bullet+}$ ions of the two isomers. The results of the investigation of this distinctive behavior of these two closely similar isomers are presented in this work.

2. Experimental

2.1. Mass spectrometry

Gas chromatography-mass spectrometry (GC-MS) analyses were carried out on a TSQ 700 triple-stage quadrupole mass spectrometer. The GC separations were carried out on a DB-5 (0.25 μm film), 6 m × 0.25 mm i.d. capillary column. The column temperature was programmed from 50 to 250 °C at 10 °C/min. EI mass spectra were obtained at 70 eV and the scan rate was 1 s^{-1}. The CI reagent gas was isobutane, and argon was used as the collision gas in CID measurements. The offset voltage was −30 V.

2.2. Materials

Mixture of **2a** and **2b** (containing also dimethyl and diethyl citraconates) was prepared by heating citraconic anhydride (20 mg, 0.18 mmol) with ethanol and methanol (0.1 ml each) and one drop of concentrated HCl at reflux for 4 h. Products were separated using GC, and structural assignment was made by the sequence of elution, based on the previously reported synthesis [1]. Isomer **2a** had a shorter retention time than **2b**.

Pairs of mixed deuterated methyl ethyl esters were prepared as mixtures by the reaction of citraconic anhydride with the appropriate deuterated alcohols.

(*Z*)- and (*E*)-2-Carbomethoxymethylidenebutyrolactone (***Z***)-**3** and (***E***)-**3**, were prepared by Wittig reaction from 2-oxobutyrolactone **4** and methoxycarbonylmethylidenetriphenylphosphorane (Scheme 2) [1].

2-Oxobutyrolactone **4** was prepared by oxidation of 2-hydroxybutyrolactone (purchased from Aldrich) using Jones reagent [10]. Jones reagent (6.5 g CrO_3 dissolved in 6 ml concentrated H_2SO_4 and 16 ml

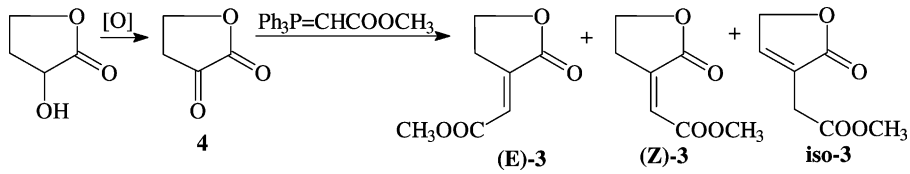

Scheme 2.

H_2O) was added dropwise to 2-hydroxybutyrolactone (5 g, 49 mmol) dissolved in 200 ml acetone in an ice bath and the mixture was stirred for 30 min in an ice bath. Methanol (50 ml) was added and stirring was continued for additional 15 min in the ice bath. The filtered solution was evaporated, and the resulting 2-oxobutyrolactone **4** was purified on a silica column using ethyl acetate:hexane (1:1) as eluent: 1.67 g, 33% yield. ^{1}H NMR: $\delta = 4.73$ (d, 2H), 6.3 (t, 1H), in agreement with previously published data [11] (in disagreement with another report [12]).

(***Z***)-**3** and (***E***)-**3**: 2-oxobutyrolactone (0.8 g, 8 mmol) was added to methoxycarbonylmethylidenetriphenylphosphorane (2.7 g, 8 mmol) dissolved in 10 ml solution of chloroform/ethanol (1:1). The solution was refluxed for 1 h. The solvent was then removed in vacuum and the concentrate was shown by GC-MS analysis to contain three isomers: (i) ***E***-**3**; (ii) ***Z***-**3**; and (iii) ***iso***-**3** (1:0.25:1 concentration ratio). The three components were separated on a silica column (1:1 ethyl acetate:hexane). ***E***-**3**: ^{1}H NMR: $\delta = 3.31$ (dt, 1H), 3.74 (s, 3H), 4.4 (t, 1H), 6.70 (t, 1H), in agreement with reported data [13a] for ***E***-**3** synthesized by a different route. ***Z***-**3**: ^{1}H NMR: $\delta = 2.98$ (dt, 2H), 3.76 (s, 3H), 4.33 (t, 2H), 6.30 (t, 1H) in agreement with reported data [13a,13b] for ***Z***-**3** synthesized by different routes. ***iso***-**3**: ^{1}H NMR: $\delta = 3.39$ (q, 1H), 3.75 (s, 3H), 4.88 (q, 1H), 7.53 (t, 1H). The analysis of the NMR data leads to the structure shown in Scheme 2.

3. Calculation details

Full geometry optimization and vibrational analysis for all species were performed using the hybrid B3LYP [14] density functional (DFT) method and the 6-31G(d,p) basis set as implemented in the Gaussian 98 series [15] of programs. Spin restricted (RB3LYP) theory has been used for singlet states, and the unrestricted form of the theory (UB3LYP) has been used for radical species. The total energies are tabulated in Table 1 along with zero-point vibration energies (ZPVE). Real vibrational frequencies confirmed the presence of minima on the potential energy surface. Transition states were identified as stationary points with one imaginary frequency. All the energies discussed in this paper are at B3LYP/6-31G(d,p)+ ZPVE.

4. Results and discussion

The 70 eV EI mass spectra of **2a** and **2b** are shown in Fig. 1. There are two major differences between the mass spectra of these two closely similar isomeric esters: (i) **2b** undergoes a more efficient elimination of methanol than **2a**: the relative abundance of the *m*/*z* 140 $[M - MeOH]^{\bullet +}$ ion is 17% for **2a** and 72% for **2b**. (ii) The $M^{\bullet +}$ ion of **2a** expels a methyl radical giving rise to the *m*/*z* 157 $[M - Me]^+$ ion (RA = 15%), which is almost absent in the EI mass spectrum of **2b**. The distinctive behavior of the two isomers is demonstrated in Scheme 3.

5. Formation of the $[M - CH_3]^+$ ion from 2a

The origin of the expelled methyl group was identified by deuterium labeling. The octa-deutero analog d_8-**2a**, in which the two alkoxycarbonyl groups are fully deuterium labeled, gives rise to the exclusive loss of a non-labeled methyl group (*m*/*z* 165, 16%). This finding clearly indicates that the two alkoxycarbonyl groups are not the origin of the expelled

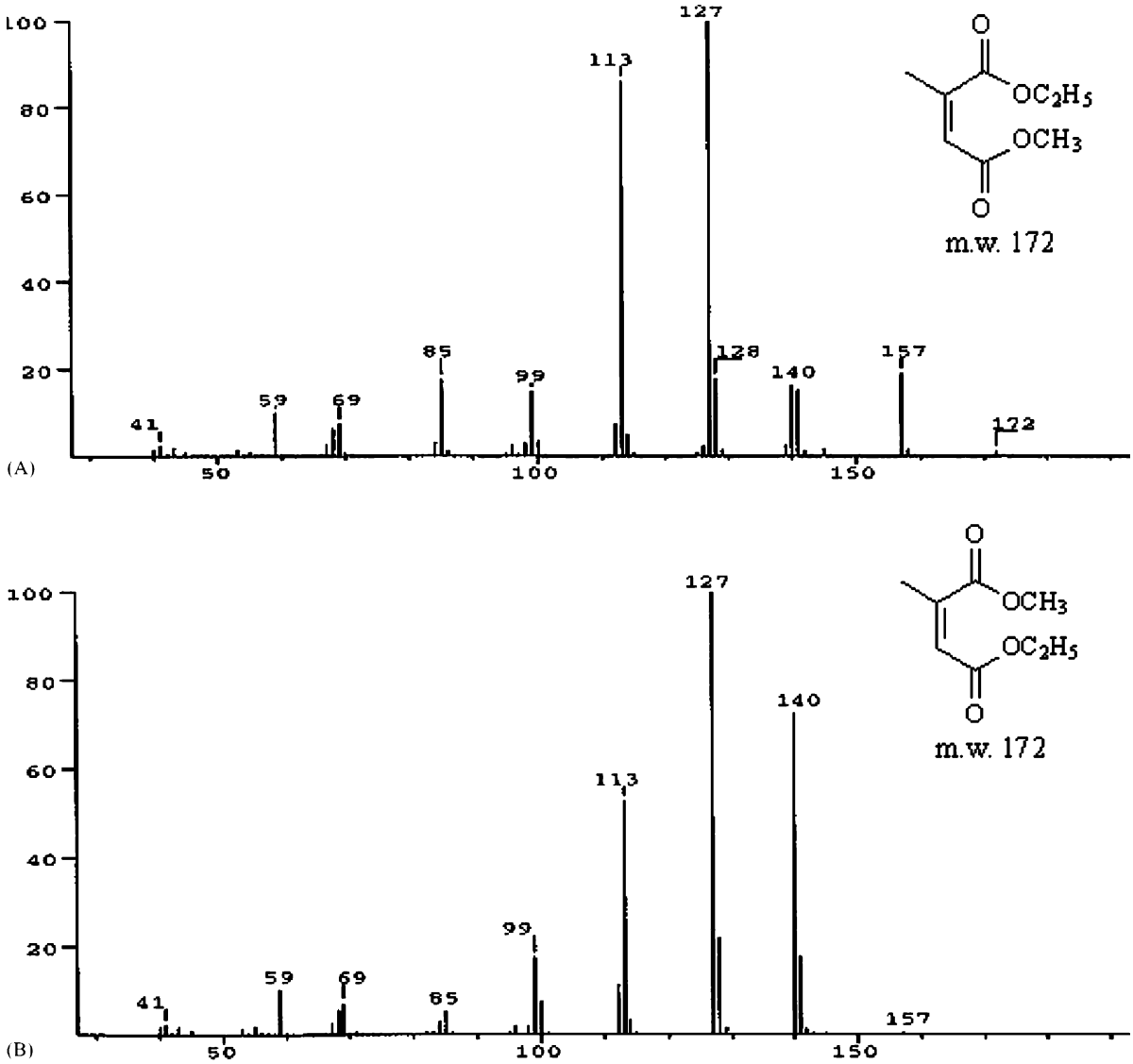

Fig. 1. EI mass spectra of **2a** (A) and **2b** (B).

methyl radical, and it is the methyl group of position 2 of the citraconic skeleton that is lost in the course of this fragmentation. The high specificity of this methyl expulsion from **2a** and the usually unfavored dissociation of vinyl bonds suggest occurrence of a multistep mechanism, that would lead to a rearranged stabilized structure of the resulting $[M-CH_3]^+$ ion.

A plausible mechanistic pathway for the methyl loss from the $M^{\bullet+}$ ion of **2a** is proposed in Scheme 4. The initial step in this mechanism is a hydrogen transfer from position 2 of the ethoxy group to the oxygen atom of the adjacent carbonyl. The resulting methylene radical (intermediate **A**) attacks the double bond at position 2 forming a five-membered lactone ring (intermediate **B**). Loss of the methyl radical, that is

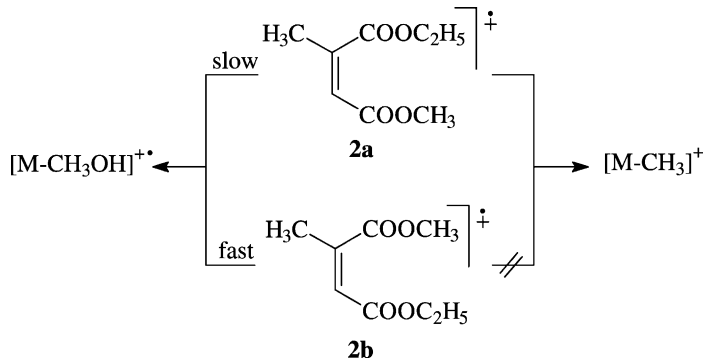

Scheme 3.

now adjacent to the radical site, forms the *m*/*z* 157 ion **a**, which has a protonated conjugated lactone-ester structure.

A collision-induced dissociation (CID) study was undertaken in order to verify the proposed structure **a** for the *m*/*z* 157 $[M - CH_3]^+$ ion. A mixture of (*Z*)- and (*E*)-2-carbomethoxymethylidene butyrolactone ((***Z***)-**3** and (***E***)-**3**)) was synthesized by Wittig reaction of 2-oxobutyrolactone and methoxycarbonylmethylidenetriphenylphosphorane (Scheme 2) and separated by column chromatography. The CID spectra of the *m*/*z* 157 MH^+ ions obtained upon isobutane-CI from (***Z***)-**3** and (***E***)-**3** are shown in Fig. 2. The geometrical isomers exhibit distinctive behavior upon CID conditions, as expected for isomeric diacid derivatives [16–18]. The (*Z*)-isomer undergoes efficient elimination of methanol (most abundant *m*/*z* 125 $[MH - MeOH]^+$ ion, 49% *m*/*z* 157 precursor ion), which is in agreement with the short distance between the ester and the lactone groups. On the other hand, the parent MH^+ ion is of highest abundance in the CID spectrum of (***E***)-**3** with the distant basic sites, and the elimination of methanol is much less efficient (45% *m*/*z* 125 $[MH - MeOH]^+$ ion).

The CID spectrum of the *m*/*z* 157 ion obtained from **2a**, shown in Fig. 2, is similar to that of (***Z***)-**3**, although the relative abundances of the secondary product ions at *m*/*z* 97 and 69 are considerably lower.

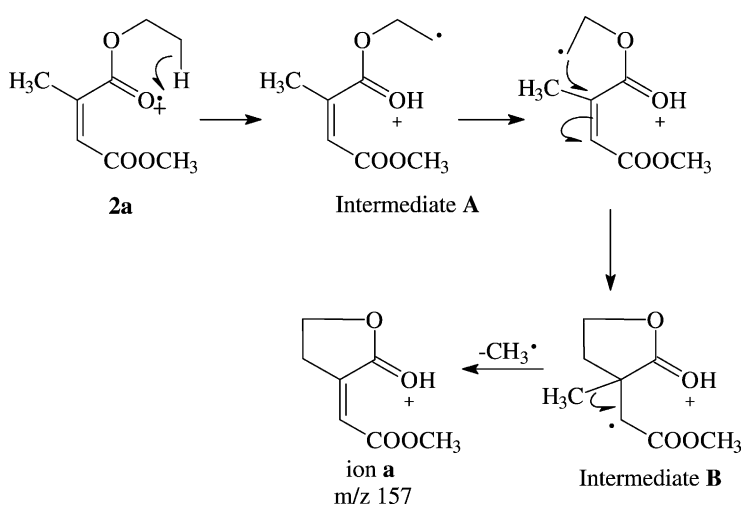

Scheme 4.

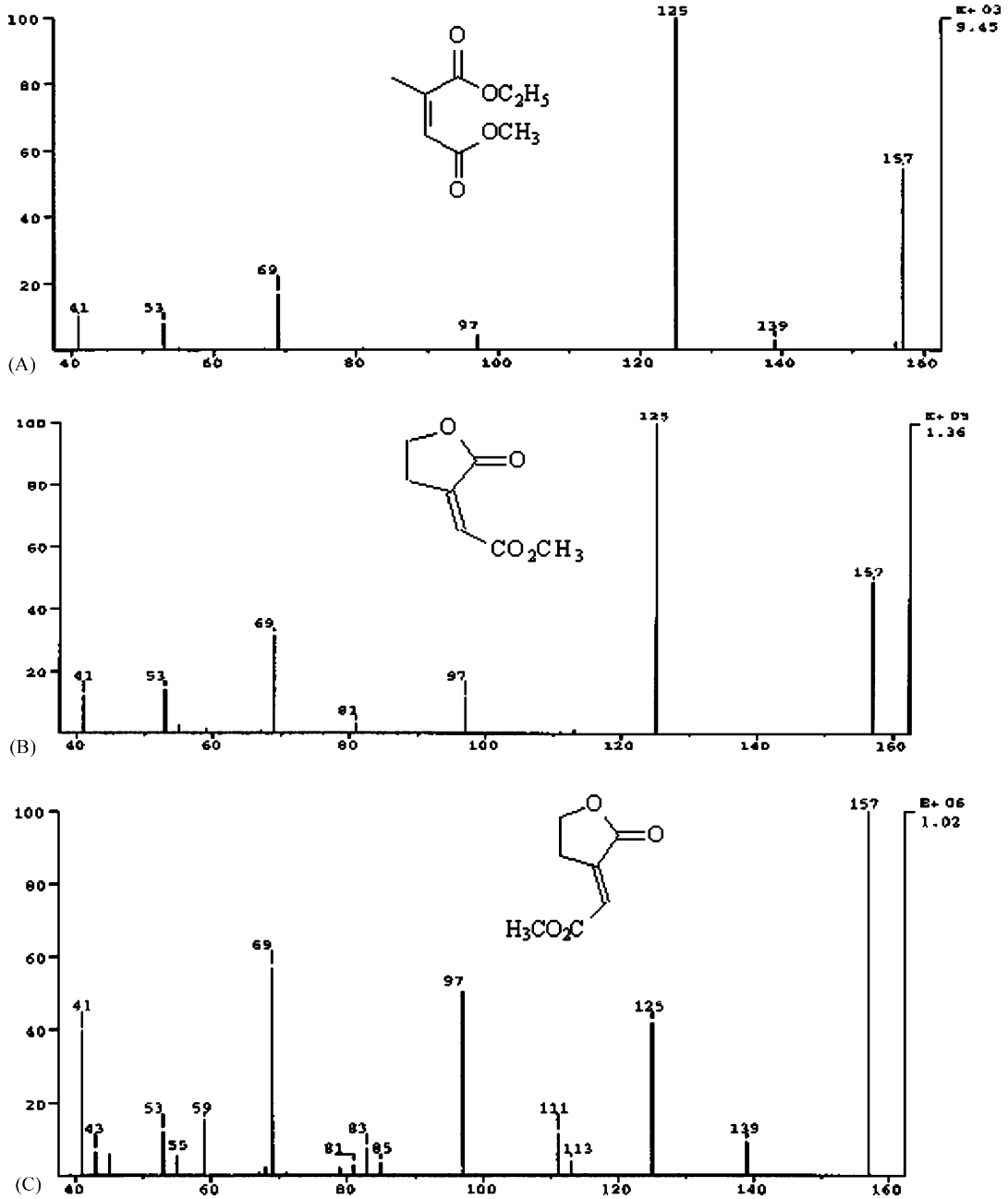

Fig. 2. CID spectra of (A) *m/z* 157 obtained from **2a**; (B) MH^+ of (***Z***)-**3**; and (C) MH^+ of (***E***)-**3**.

This finding suggests the structure of (***Z***)-**3** for the great part of *m/z* 157 ions obtained from **2a**. The low abundance of the *m/z* 139 $[P–H_2O]^+$ ion in the CID spectrum (1%) indicates low contribution of (***E***)-**3**, where that product ion is of considerable abundance (10%). The preferential formation of the (*Z*)-isomer results from its stabilization by proton bridging between the two adjacent carbonyl groups. The quantitative

differences between the two CID spectra (*m*/*z* 157 of **2a** vs. MH^+ of (***Z***)-**3**) may be due to the different energy content of the precursor ions, which are obtained under different conditions (EI-induced fragmentation of **2a** vs. CI protonation of (***Z***)-**3**). The above result supports the mechanistic pathway proposed in Scheme 4 for the stepwise expulsion of the methyl radical from the $M^{\bullet+}$ ion of **2a**.

We will turn now to the question of the isomer specificity of the loss of the methyl radical, which takes place in **2a** but not in **2b**. In analogy to the initial step in the mechanistic pathway proposed above for **2a**, a similar hydrogen migration in **2b** from the ethyl moiety to the adjacent carbonyl oxygen atom would form a radical site at C2 of the original ethoxy group (see Scheme 5). Cyclization by bond formation between the latter methylene radical and C2 of the citraconic skeleton could give rise to intermediate **D**, which would be expected to undergo expulsion of a methyl and/or a methoxycarbonyl radical. The absence of the *m*/*z* 157 $[M - CH_3]^+$ ion in the EI mass spectrum of **2b** could be attributed to the preferential expulsion of the methoxycarbonyl radical affording the *m*/*z* 113 $[M - CH_3OCO]^+$ ion, which is one of the abundant ions (RA 60%) formed from **2b**. However, the *m*/*z* 113 ion is also present in the mass spectrum of **2a**, and its abundance is even higher than that in **2b** (RA 90%). Moreover, the CID mass spectra of the *m*/*z* 113 ions obtained from **2a** and **2b** are very similar (see Fig. 3), which is indicative of identical structures. Therefore, there is no evidence for the cyclization step leading to intermediate **D**.

There is a possibility of differentiation of the two proposed cyclization steps affording intermediate **B** from **2a** (Scheme 4) and intermediate **D** from **2b** (Scheme 5) based on Baldwin rules in the condensed phase [19–21]. The formation of intermediate **B** from **2a** is defined as a 5-*exo-trig* ring closure, while **D** would be formed by a 6-*endo-trig* process. For radical trigonal ring closures 5-*exo-trig* processes are favored while 6-*endo-trig* analogs are disfavored. However, both 5-*exo-trig* and 6-*endo-trig* are favored in cationic cyclizations [19]. If the gas phase radical cation chemistry resembles the radical behavior in the condensed phase, Baldwin rules would favor formation of intermediate **B** by the 5-*exo* cyclization of intermediate **A**, but disfavor the 6-*endo* ring closure to form intermediate **D** from **C**, and thus explain the absence of the *m*/*z* 157 $[M - CH_3]^+$ ion in the mass spectrum of **2b**. It is of course possible that the reluctance of **2b** to expel the methyl radical is due to the competition of this process with the elimination of methanol, which is much more efficient in **2b** than in **2a**.

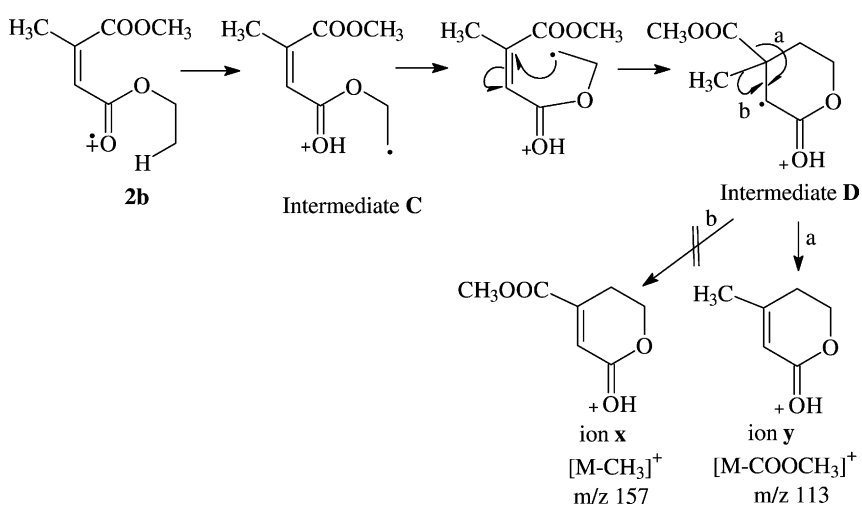

Scheme 5.

Table 1
Computed energies

Structure	Total electronic energies (Hartrees)	ZPVE (kcal/mol)	Relative energies (kcal/mol)
Intermediate **B**	−612.70651	123.05	0[a]
2a$^{\bullet+}$	−612.67034	122.44	22.1[a]
TS-1	−612.63983	118.57	37.4[a]
Intermediate **A**	−612.65815	121.03	28.3[a]
TS-2	−612.65349	120.2	30.4[a]
Ion **a**	−572.82791	98.33	16.4[a,b]
Intermediate **D**	−612.71137	124.2	0[c]
2b$^{\bullet+}$	−612.68393	122.46	15.5[c]
TS-3	−612.64954	121.58	31.3[c]
Intermediate **C**	−612.66557	120.80	15.4[c]
TS-4	−612.65186	118.17	49.6[c]
Ion **x**	−572.81519	100.17	28.3[c,b]
Ion **y**	−384.26986	90.74	23.0[c,d]
$CH_3^{\bullet}$	−39.84288	18.68	
$CH_3OCO^{\bullet}$	−228.40060	30.75	
Ion $\mathbf{c}_{11}$	−496.93367	88.60	0[e]
Ion $\mathbf{b}_{11}$	−496.91899	88.70	9.3[e]
Intermediate $\mathbf{C}_{11}$	−496.90841	85.91	13.2[e]
Intermediate $\mathbf{A}_{11}$	−496.90609	85.83	14.5[e]
Ion $\mathbf{c}_2$	−496.88553	87.16	28.8[e]
Ion $\mathbf{b}_2$	−496.88134	86.37	30.6[e]

[a] Energies relative to intermediate **B**.
[b] The energy of methyl radical is included.
[c] Energies relative to intermediate **D**.
[d] The energy of methoxycarbonyl radical is included.
[e] Energies relative to ion $\mathbf{c}_{11}$.

Quantum mechanical calculations have been performed in order to find explanation for the different behavior of the M$^{\bullet+}$ ions of **2a** and **2b**. The results of the calculations are listed in Table 1, and the structures of calculated species are shown in Fig. 4a and b. The potential energy profile calculated for the loss of CH_3 radical from ionized **2a**, shown in Fig. 5a, is in agreement with the mechanistic pathway proposed in Scheme 4. The rate determining step in this process is the hydrogen transfer from carbon 2 of the ethoxycarbonyl group to the adjacent carbonyl oxygen, and the barrier energy of this rearrangement is 15.3 kcal/mol. The formation of intermediate **B** from intermediate **A** is exothermic (28.3 kcal/mol), and the energy barrier for this transformation is very low (2.1 kcal/mol).

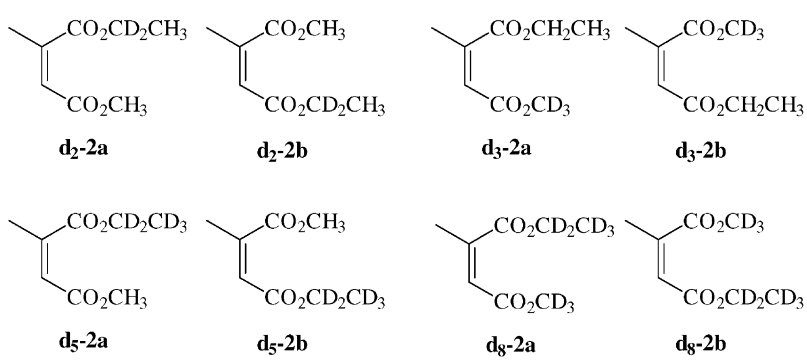

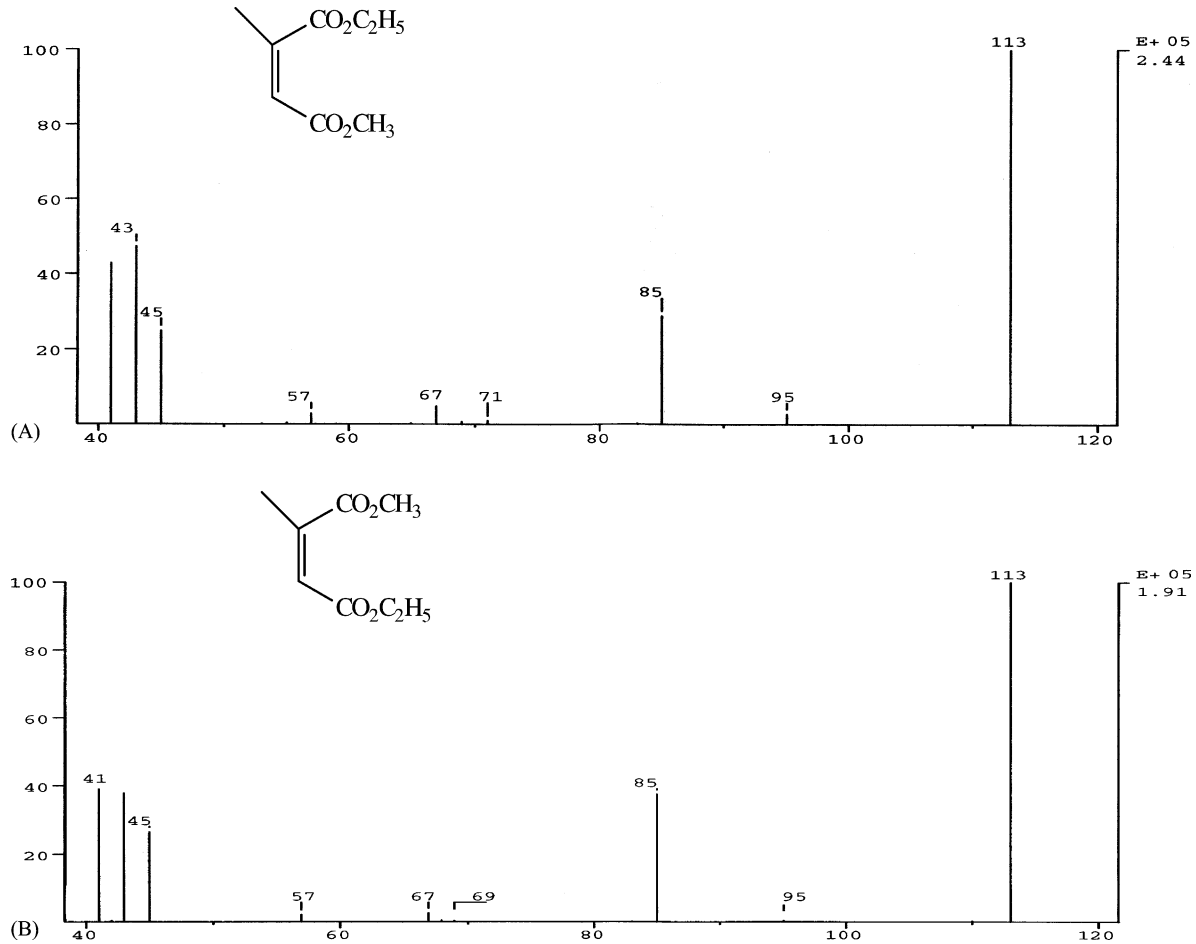

Fig. 3. CID of *m/z* 113 ions obtained from **2a** (A) and **2b** (B).

The energy profile calculated for the mechanistic pathway, proposed in Scheme 5 for the unobserved loss of CH_3 radical from the $M^{\bullet+}$ ion of **2b**, is shown in Fig. 5b. The formation of intermediate **D** from intermediate **C** by *endo*-6 cyclization is exothermic (15.4 kcal/mol), but the energy of the transition state TS-4 of this transformation is very high (49.6 kcal/mol, barrier energy 34.2 kcal/mol). The great difference between the calculated barrier energies of the *exo*-5 and *endo*-6 cyclizations (2.1 kcal/mol vs. 34.2 kcal/mol, respectively), leading to intermediates **B** and **D**, respectively, provides an explanation for the different behavior of the two isomers **2a** and **2b** with respect to the elimination of the methyl radical. If intermediate **D** were formed, it would have readily eliminated the methyl radical from position 2: the calculated energy of this dissociation is 28.3, 12.9 kcal/mol higher than the energy of intermediate **C**. The absence of the *m/z* 157 $[M - CH_3]^+$ ion in the mass spectrum of **2b** is thus in agreement with high barrier energy involved in the formation of intermediate **D**.

6. Elimination of methanol

The loss of methanol from the $M^{\bullet+}$ ions of **2a** and **2b** was studied by deuterium labeling. Pairs of the

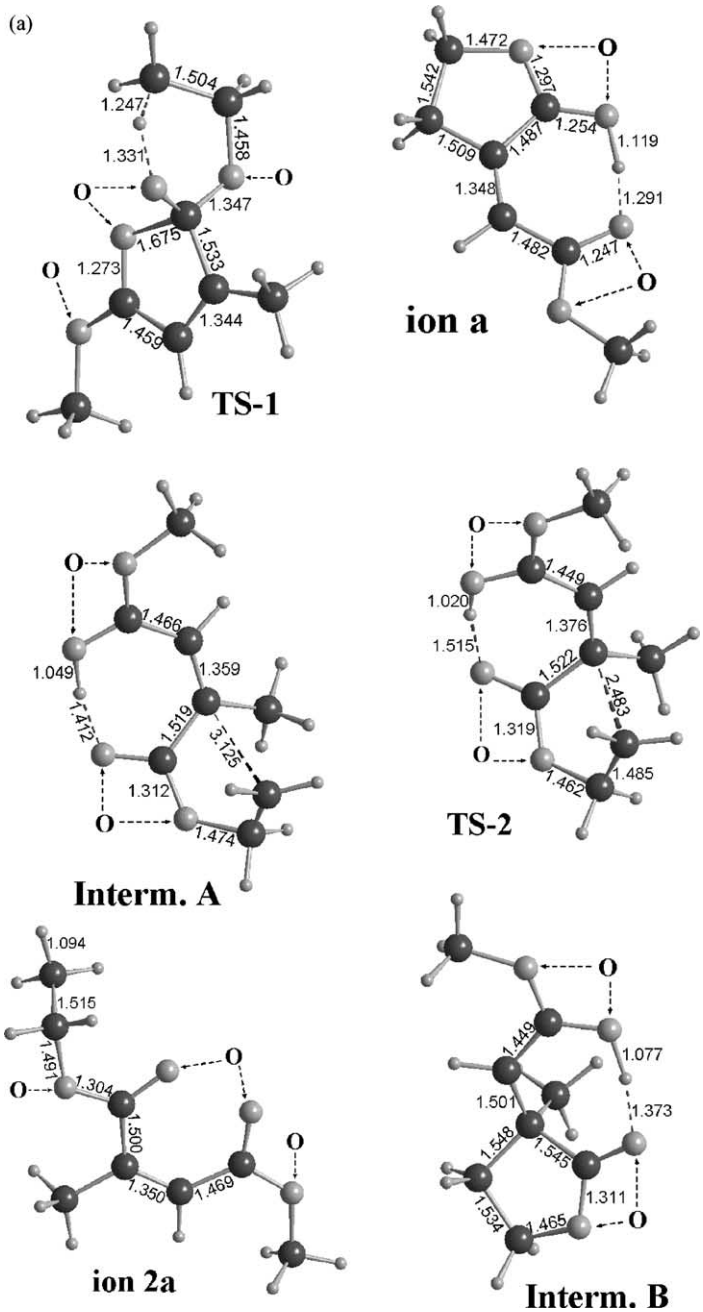

Fig. 4. (a) Computed structures involved in the loss of CH_3 radical from the molecular ion of **2a**. (b) Computed structures involved in the unobserved loss of CH_3 radical from the molecular ion of **2b**.

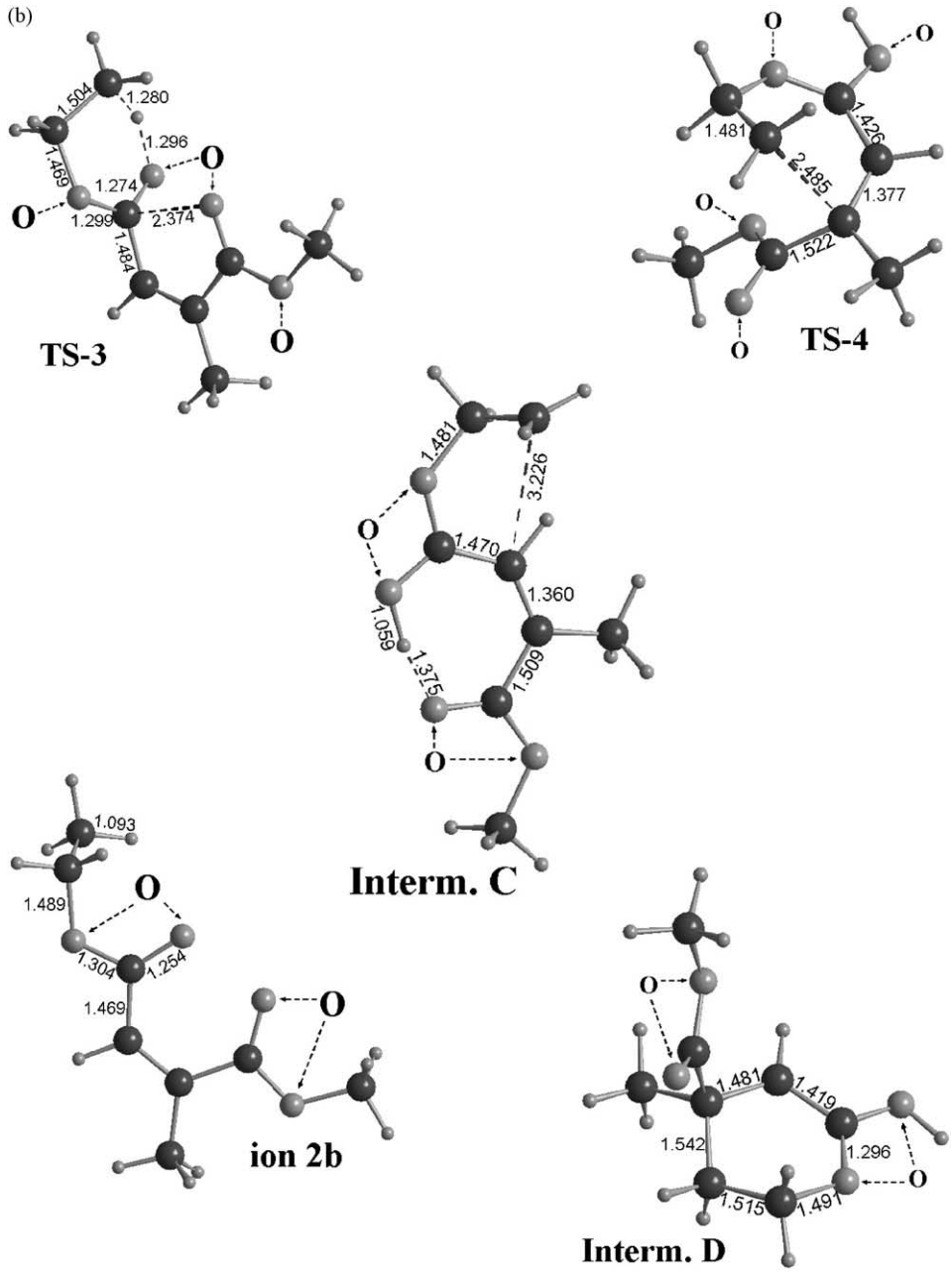

Fig. 4. (*Continued*).

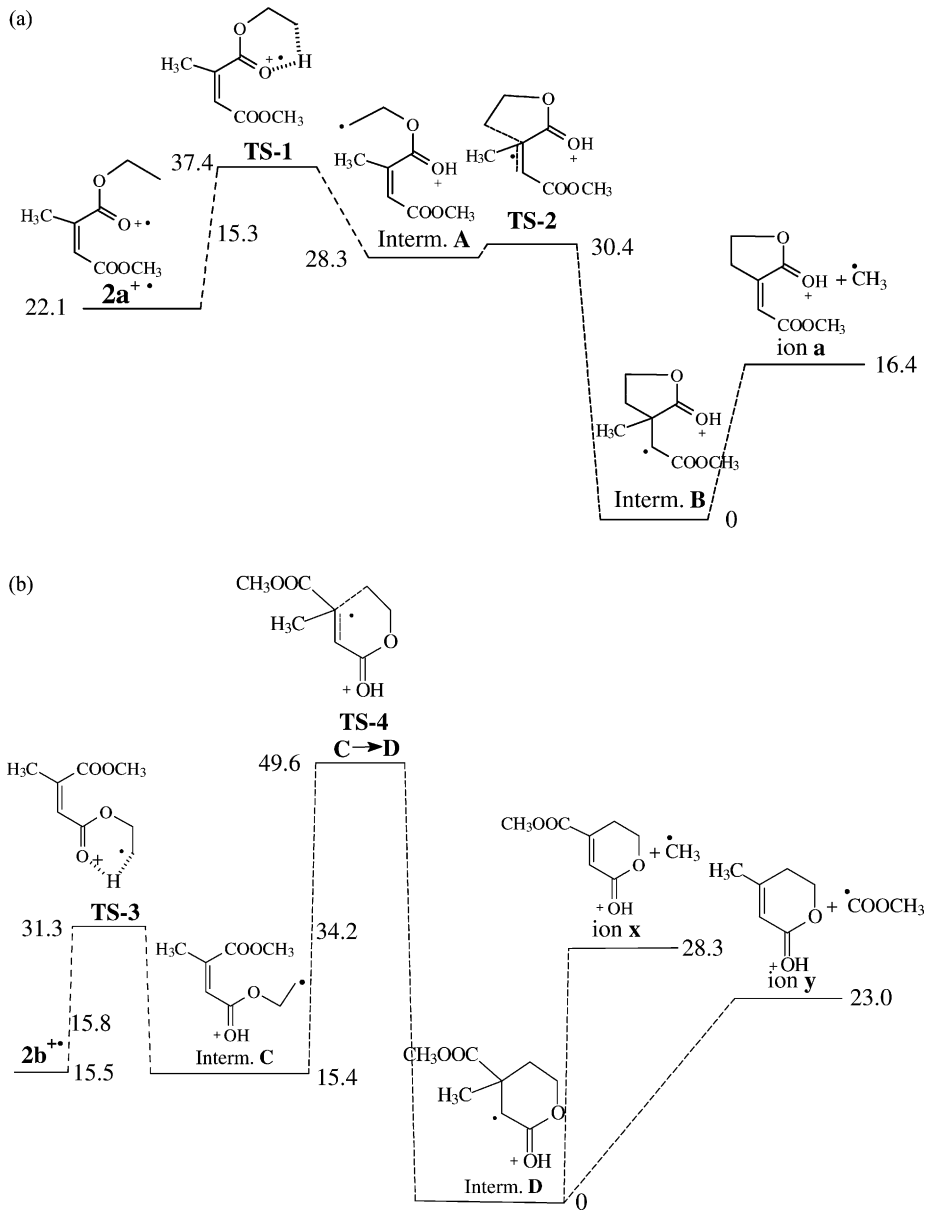

Fig. 5. (a) Calculated energy profile (kcal/mol) for the formation of the $[M - CH_3]^+$ ion from the molecular ion of **2a**. (b) Calculated energy profile (kcal/mol) for the unobserved formation of the $[M - CH_3]^+$ ion from the molecular ion of **2b**.

deuterated isomeric mixed esters d_2-**2a**, d_2-**2b**, d_3-**2a**, d_3-**2b**, d_5-**2a**, d_5-**2b**, d_8-**2a** and d_8-**2b** were prepared and their EI mass spectra were measured. The relative abundances of the $[M - \text{methanol}]^{\bullet+}$ ions are summarized in Table 2.

The data in Table 2 clearly show that the elimination of methanol takes place in both isomers with the abstraction of a hydrogen atom from position 2 of the ethoxycarbonyl group. This finding suggests that the elimination is preceded by hydrogen migration

Table 2
Elimination of methanol from deuterium labeled citraconates (%RA)

	$[M - MeOH]^{\bullet+}$	$[M - MeOD]^{\bullet+}$	$[M - CD_3OH]^{\bullet+}$	$[M - CD_3OD]^{\bullet+}$
2a	17			
2b	72			
d_2-**2a**	12[a]	–[b]		
d_2-**2b**	37[a]	–[b]		
d_3-**2a**			10	
d_3-**2b**			49	
d_5-**2a**	–[b]	15		
d_5-**2b**	–[b]	53		
d_8-**2a**			–[b]	12
d_8-**2b**			–[b]	43

[a] Measured under different conditions with TSQ 700.
[b] Less than 1%.

from that position to the oxygen atom of the adjacent carbonyl, forming intermediate **A** (open-chain $\mathbf{A}_1$ or ring-closed $\mathbf{A}_{11}$) in the case of **2a** (which has been previously proposed to precede the expulsion of CH_3 radical, see Scheme 4), and intermediate **C** (open-chain $\mathbf{C}_1$ or ring-closed $\mathbf{C}_{11}$) in the case of **2b**. Plausible mechanistic pathways for the loss of methanol from **2a** and **2b** are proposed in Schemes 6 and 7, respectively.

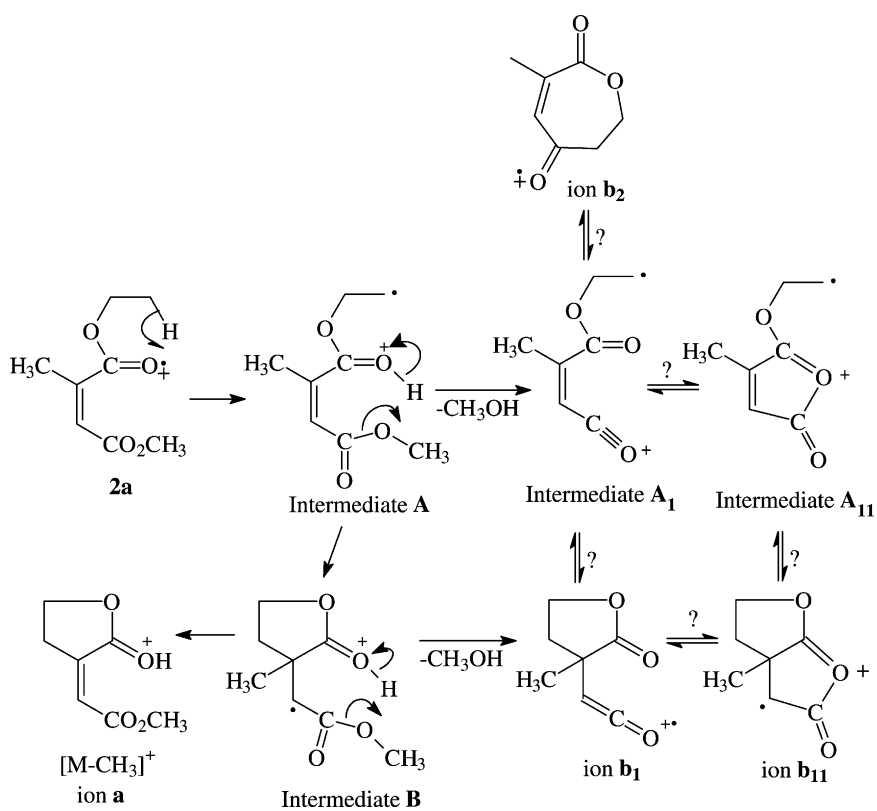

Scheme 6.

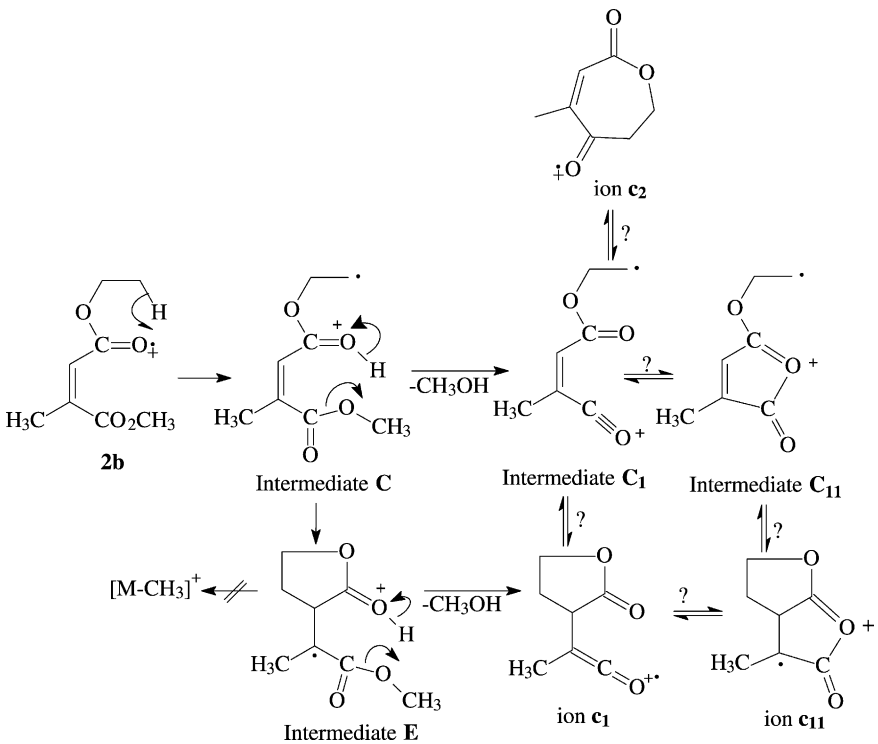

Scheme 7.

The elimination of methanol from the $M^{\bullet+}$ ions of **2a** and **2b** may take place via cyclization of intermediates **A** and **C** to **B** and **E**, respectively, resulting in the ionized ketene structures $\mathbf{b}_1$ and $\mathbf{c}_1$. Another possibility is a direct elimination of methanol from the acyclic intermediates **A** and **C**, which may be followed by cyclization to the seven-membered ketolactone structures $\mathbf{b}_2$ and $\mathbf{c}_2$, respectively. The pronounced preference of methanol elimination from **2b** may be attributed to the presumably greater stability of the more

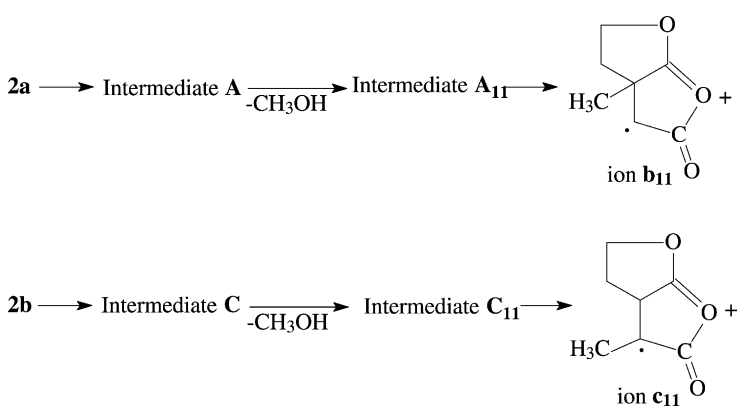

Scheme 8.

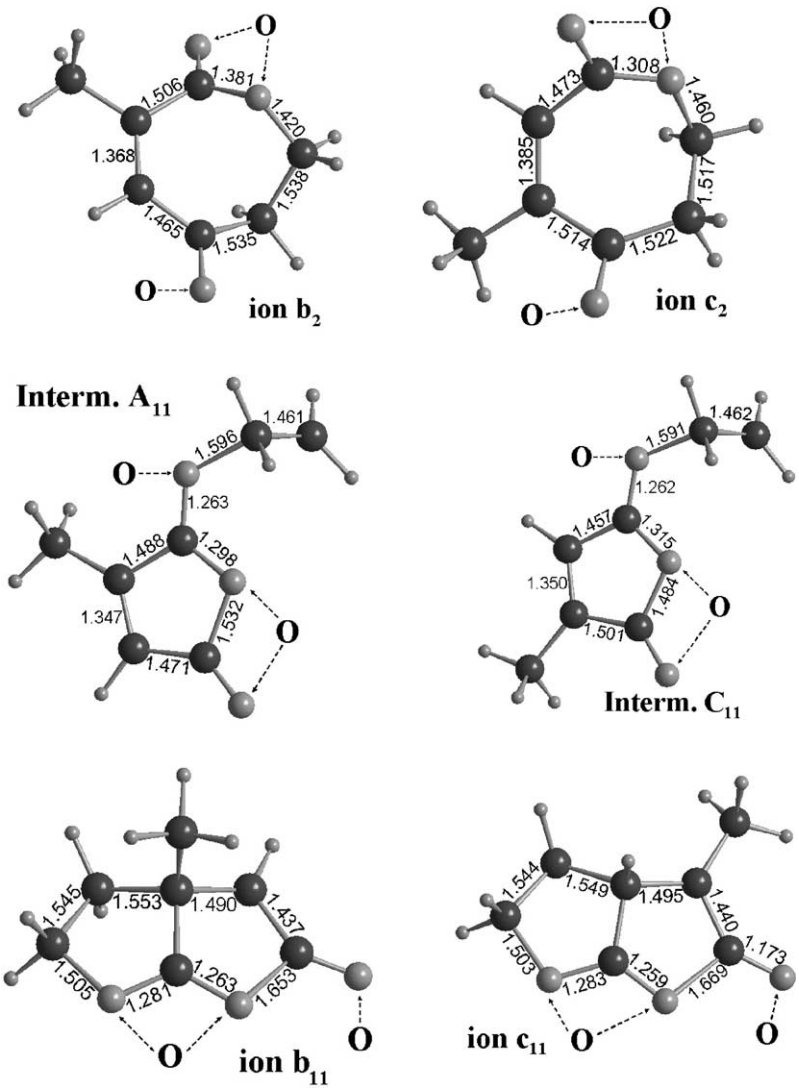

Fig. 6. Computed structures involved in the elimination of methanol from the molecular ions of **2a** and **2b**.

substituted ketene structure of ion $\mathbf{c}_1$ (or of its cyclic analog $\mathbf{c}_{11}$), as compared with ion $\mathbf{b}_1$ (or cyclized $\mathbf{b}_{11}$) obtained from **2a**. An alternative (or additional) origin of the suppressed methanol elimination from **2a** is the competitive expulsion of the methyl radical from intermediate **B**, which is not possible in intermediate **E**.

DFT calculations were performed for the species proposed in Schemes 6 and 7. The results of the calculations are listed in Table 1, the computed ion structures are shown in Fig. 6 and the resulting energy profile is given in Fig. 7. The elimination of methanol from **2a** and **2b** via intermediates **A** and **C**, respectively (for their computed energies see Figs. 5a and b) gives rise to the cyclized intermediates $\mathbf{A}_{11}$ and $\mathbf{C}_{11}$, respectively. The calculations suggest that the open-chain structures $\mathbf{A}_1$ and $\mathbf{C}_1$ are unstable. The formation of the seven-membered ring ions $\mathbf{b}_2$

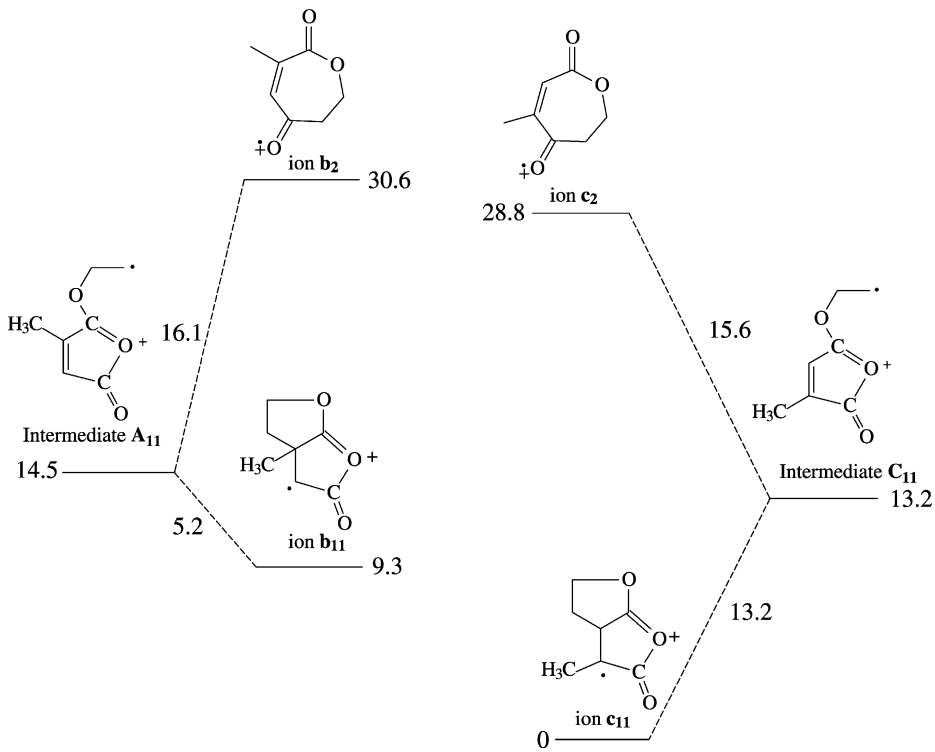

Fig. 7. Calculated energy profile (kcal/mol) for the elimination of methanol from the molecular ions of **2a** and **2b**.

and $\mathbf{c}_2$ from intermediates $\mathbf{A}_{11}$ and $\mathbf{C}_{11}$, respectively, is an endothermic process (16.1 and 15.6 kcal/mol, respectively), while the transformation of the two intermediates to the bicyclic isomeric ions $\mathbf{b}_{11}$ and $\mathbf{c}_{11}$ is exothermic in both cases. The considerably greater exothermicity of the formation of ion c_{11}, as compared with $\mathbf{b}_{11}$ (13.2 kcal/mol vs. 5.2 kcal/mol), provides an explanation for the greater efficiency of methanol elimination from **2b** than from **2a**. The information derived from the DFT calculations, concerning the elimination of methanol from the $M^{\bullet+}$ of **2a** and **2b**, is summarized in Scheme 8.

7. Conclusion

We have shown in this work that the two closely similar isomeric methyl ethyl citraconates exhibit a remarkably different behavior upon EI. This result may find use in structural assignments of analogous isomers which exhibit very similar IR and NMR spectra. As in other previously reported cases, the different behavior of the isomeric mixed ethyl methyl esters has led to a better understanding of the gas phase chemistry of this system, which could not be achieved on the examination of the symmetrical analogs. Thus, in the citraconate system, the molecular ion of the diethyl ester **2c** expels a methyl radical while the dimethyl ester **2d** does not. The mechanistic pathway proposed for the specific loss of a methyl radical from **2a** (shown in Scheme 4) but not from the isomeric **2b**, provides a simple explanation for the different behavior of **2c** and **2d**.

An additional noteworthy point in this work is the demonstration of the ability of mass spectrometry to differentiate and assign structures of the geometrically isomeric (*Z*)- and (*E*)-2-carbomethoxymethylidene butyrolactones (***Z***)-**3** and (***E***)-**3**. This finding suggests

that the structural assignment of *cis*-diesters based on alcohol elimination from their protonated molecules [16–18] may be extended to lactone-ester systems, and possibly to other appropriate diacid derivatives.

Acknowledgements

This work was supported by the Fund for Promotion of Research at the Technion. We are grateful to Dr. Y.S. Balazs for assistance in NMR measurements.

References

[1] D. Bornstein, A. Weisz, A. Mandelbaum, Org. Mass Spectrom. 21 (1986) 225.
[2] A. Weisz, M. Cojocaru, A. Mandelbaum, J. Chem. Soc. Commun. (1989) 331.
[3] A. Mandelbaum, A. Weisz, M. Cojocaru, Adv. Mass Spectrom. 11 (1989) 598.
[4] A. Mandelbaum, D.R. Mueller, W.J. Richter, I. Vidavsky, A. Weisz, Org. Mass Spectrom. 24 (1989) 857.
[5] A. Mandelbaum, D.R. Mueller, W.J. Richter, I. Vidavsky, Int. J. Mass Spectrom. Ion Process. 10 (1990) 565.
[6] I. Vidavsky, A. Mandelbaum, T. Tamiri, S. Zitrin, Org. Mass Spectrom. 26 (1991) 287.
[7] D. Bornstein, A. Mandelbaum, I. Vidavsky, B. Domon, D.R. Mueller, W.J. Richter, Org. Mass. Spectrom. 26 (1991) 793.
[8] D. Bornstein, A. Mandelbaum, I. Vidavsky, B. Domon, D.R. Mueller, W.J. Richter, Org. Mass. Spectrom. 28 (1993) 230.
[9] A. Mandelbaum, D. Bornstein, T. Tamiri, S. Zitrin, in: Proceedings of the 35th ASMS Annual Conference on Mass Spectrometry and Allied Topics, Denver, CO, 4–9 May, 1987, p. 854.
[10] R.A. Leppik, Steroids 41 (1983) 475.
[11] M. Verny, R. Vessier, Bull. Soc. Chem. France (1969) 1729.
[12] H.H. Wasserman, J.L. Ives, J. Org. Chem. 43 (1978) 338.
[13] Y. Jenkitkasemwong, Y. Thebtaranonth, N. Wajirum, Tetrahedron Lett. (1979) 1615;
(b) G. Bartolo, G. Salerno, F. De Pascali, M. Costa, G.P. Chiusoli, J. Chem. Soc., Perkin Trans. (1997) 147.
[14] (a) C. Lee, W. Young, R.G. Parr, Phys. Rev. B 73 (1988) 785;
(b) A.D. Becke, J. Chem. Phys. 98 (1993) 5648.
[15] M.J. Frisch, G.W. Trucks, H.B. Schlegel, G.E. Scuseria, M.A. Robb, J.R. Cheeseman, V.G. Zakrzewski, J.A. Montgomery Jr., R.E. Stratmann, J.C. Burant, S. Dapprich, J.M. Millam, A.D. Daniels, K.N. Kudin, M.C. Strain, O. Farkas, J. Tomasi, V. Barone, M. Cossi, R. Cammi, B. Mennucci, C. Pomelli, C. Adamo, S. Clifford, J. Ochterski, G.A. Petersson, P.Y. Ayala, Q. Cui, K. Morokuma, N. Rega, P. Salvador, J.J. Dannenberg, D.K. Malick, A.D. Rabuck, K. Raghavachari, J.B. Foresman, J. Cioslowski, J.V. Ortiz, A.G. Baboul, B.B. Stefanov, G. Liu, A. Liashenko, P. Piskorz, Komaromi, R. Gomperts, R.L. Martin, D.J. Fox, T. Keith, M.A. Al-Laham, Y. Peng, A. Nanayakkara, M. Challacombe, P.M.W. Gill, B. Johnson, W. Chen, M.W. Wong, J.L. Andres, C. Gonzalez, M. Head-Gordon, E.S. Replogle, J.A. Pople, Gaussian 98, Revision A.11.3, Gaussian, Inc., Pittsburgh, PA, 2002.
[16] A.G. Harrison, Chemical Ionization Mass Spectrometry, 2nd ed., CRC Press, Boca Raton, FL, 1992, pp. 178–181, and references cited therein.
[17] A. Weisz, A. Mandelbaum, J. Shabanowitz, D.F. Hunt, Org. Mass Spectrom. 19 (1984) 238.
[18] A. Etinger, A. Idina, A. Mandelbaum, J. Am. Chem. Soc. 115 (1993) 7397.
[19] J.E. Baldwin, J. Chem. Soc. Chem. Commun. (1976) 734.
[20] J.E. Baldwin, J. Cutting, W. Dupont, L. Kruse, L. Silberman, R.C. Thomas, J. Chem. Soc. Chem. Commun. (1976) 736.
[21] A. Padwa, H. Nimmesgern, G.S. Wong, J. Org. Chem. 50 (1985) 560.